Sensors & Actuators: B. Chemical 367 (2022) 132117

Contents lists available at ScienceDirect

Sensors and Actuators: B. Chemical

journal homepage: www.elsevier.com/locate/snb

General analysis method for the signal enhancement of microwave gas sensor though variation of energy loss

Nan Zhang [a], Bin Jiang [a], Shanshan Xue [a], Xiaolong Wang [a,b,*], Tianshuang Wang [c], Peng Sun [a], Geyu Lu [a,b]

[a] State Laboratory of Integrated Optoelectronics, College of Electronic Science and Engineering, Jilin University, 2699 Qianjin Street, Changchun 130012, People's Republic of China
[b] International Center of Future Science, Jilin University, 2699 Qianjin Street, Changchun 130012, People's Republic of China
[c] State Key Laboratory of Inorganic Synthesis and Preparative Chemistry, College of Chemistry, Jilin University, Changchun 130012, People's Republic of China

ARTICLE INFO

Keywords:
Dielectric loss tangent
Graphite powder
Permittivity variation
Microwave gas sensor
Ammonia

ABSTRACT

Microwave gas sensor (MGS) becomes a highlight recently because it can work at the room temperature (20 ℃) and has potential wireless application. However, there are still some problems such as low sensitivity and linearity. In this short communication, a novel analysis method based on variation of energy loss was proposed as sensor response for the first time. The as-prepared device is successfully used for NH_3 detection based on commercial graphite powder which can achieve a low detection limit (1 ppm, 20 ℃), excellent selectivity and humidity-resistance (20–95% RH). Moreover, the sensor shows good linearity for low concentration range of NH_3 from 1 to 5 ppm ($R^2 = 0.999$) or high concentration range from 10 to 200 ppm ($R^2 = 0.99$) through analyzing energy loss calculated by both reflection and transmission, which is more linear compared with that only using reflection or transmission. Therefore, this study provides a simple and universal method for response signal analysis, which can amplify the weak sensing signal then realize high-performance MGS.

1. Introduction

Carbon-based material, such as graphene [1] and carbon nanotube (CNT) [2] are widely used in gas sensor due to its high carrier mobility and sensitive electrical conductance to target gas. However, high cost and poor repeatability limit their commercial application. Compared with graphene and CNT, graphite powder (GP) is more appropriate for commercial application due to the lower price, easier preparation, and better repeatability. GP has been applied in anode material of lithium-ion batteries [3], high-temperature gas-cooled reactors [4] and fast neutrons moderator [5] in nuclear engineering, and good solid lubricant [6]. However, there are little reports about chemiresistor gas sensor based on GP, because the specific surface area of GP is small and the response is rather limited for non-functionalized GP [7].

Microwave gas sensor (MGS) has become a highlight in recent research owing to the novel sensitive mechanism which can realize high sensitivity at the room temperature [8–15]. Comparing with traditional gas sensors [16], MGS can realize gas detection by variation of microwave signal. There are two parts, including microwave circuit and sensitive material, which determine sensing performance. The sensitive material is applied on crucial area of microwave circuit. Especially, because the large and rough surfaces of carbon-based materials are beneficial for gas adsorption and diffusion, carbon-based materials [8–10] seem to have better sensing performance than semiconductor oxides [11–14] and organic matter [15]. About the circuit design, the microwave antenna can only test reflection (S_{11}) under different gas concentration with the absence of transmission signal (S_{21}) [11]. Moreover, the quality factor (Q-factor) of antenna is relatively low, which will reduce sensitivity. For increasing Q-factor and analyzing microwave signal completely, the complementary split-ring resonator (CSRR) as basic functional unit of metamaterial is applied for MGS [8]. Nevertheless, CSRR is located on the bottom of circuit, which will increase the insertion loss and fabrication difficulty. As a result, the planar microwave resonators, such as interdigital capacitor resonators [12,14,15], spiral resonator [13], and split-ring resonator (SRR) [9] are designed for MGS. Among them, SRR has relative high Q-factor and region of highly concentrated electric field. Therefore, MGS consisting of SRR can exhibit enhanced sensitivity and linearity and be an ideal

* Corresponding author at: State Laboratory of Integrated Optoelectronics, College of Electronic Science and Engineering, Jilin University, 2699 Qianjin Street, Changchun 130012, People's Republic of China.
E-mail address: brucewang@jlu.edu.cn (X. Wang).

https://doi.org/10.1016/j.snb.2022.132117
Received 29 April 2022; Received in revised form 19 May 2022; Accepted 24 May 2022
Available online 26 May 2022

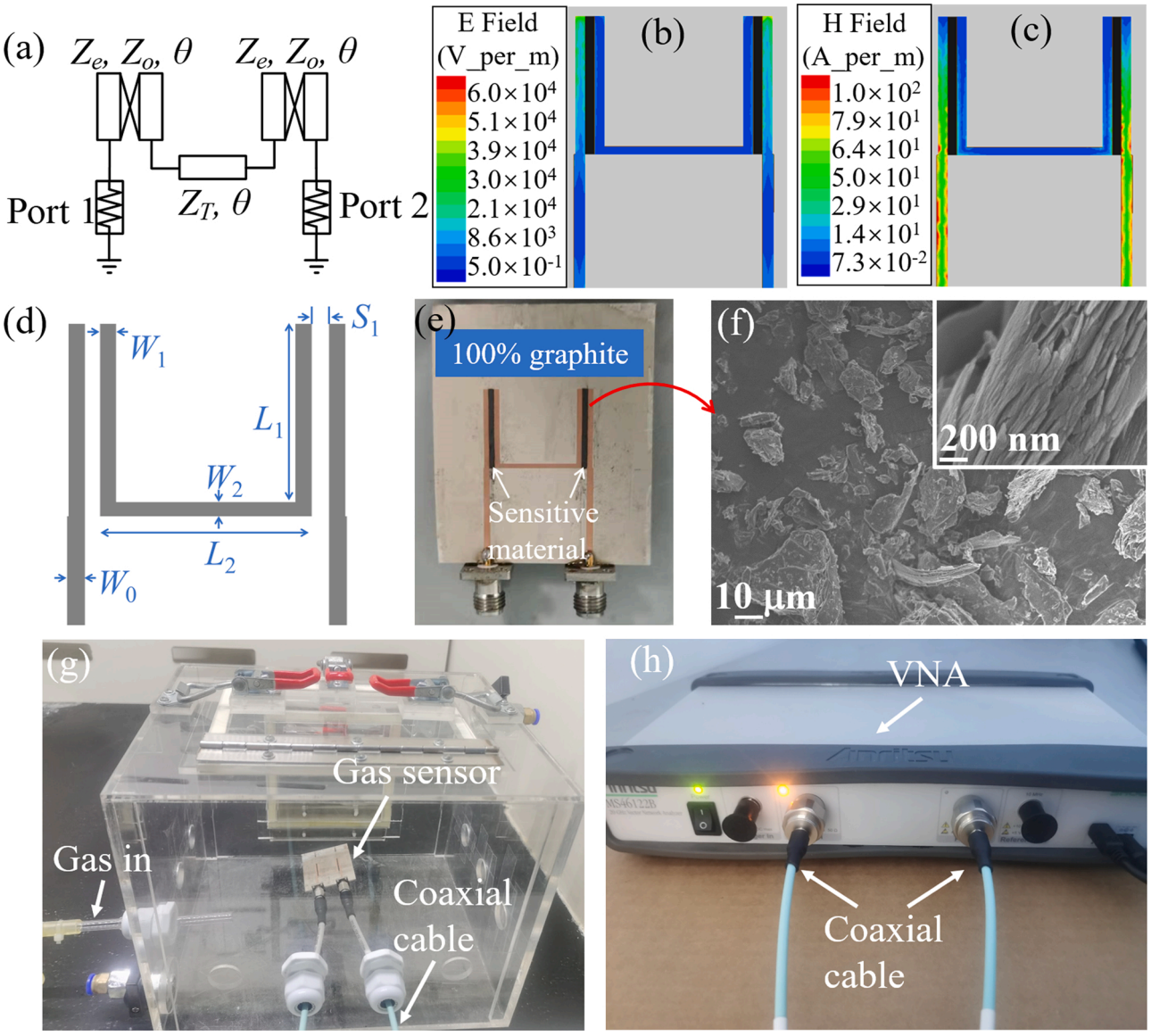

Fig. 1. (a) Topology of proposed BSF; (b) electric and (c) magnetic field intensity of the MGS simulated by HFSS; (d) layout of proposed BSF; (e) photograph of fabricated MGS; (f) SEM image of commercial GP; The photograph of (g) 10 L gas chamber and (h) VNA used in this work.

choice for gas sensing. However, the region of concentrated electric field is located on ring gap, which is compact and can only coat limited sensing materials. Recently, we have improved the gas sensing properties by designing the coupled-lines resonator (CLR) [10]. Compared with other resonators [9,12–15], CLR has appropriate coating area, concentrated electromagnetic field, and simple structure, which make it more suitable for high-performance MGS design. Therefore, it is meaningful to combine the CLR and commercial GP for the fabrication of high-performance MGS.

Here we for the first time utilize variation of energy loss as sensor response signal for MGS. Aiming at NH_3 detection, commercial GP is selected as sensitive material coated in the gaps of CLRs. The gas sensing investigation indicates that proposed MGS has high sensitivity, good selectivity, well linearity and humidity-resistance through analyzing the energy loss calculated by both S_{11} and S_{21}. Compared with our previous work [10], there are three unique features: (1) The detection limit is improved from 10 ppm to 1 ppm based on the same circuit and simpler sensitive material; (2) The linearity of response is enhanced by using proposed novel analysis method; (3) The sensing mechanism based on dielectric constant loss is proposed and verified in the final part of this work.

2. Experimental

As shown in Fig. 1a, the narrow band-stop filter (BSF) consisting of two CLRs and single transmission line was designed as MGS circuit. Z_e and Z_o are the even- and odd-mode characteristic impedances of CLRs, and Z_t is the characteristic impedance of transmission line. All electrical lengths θ are equal to 90° at the center frequency 2 GHz. The design parameters are $Z_e = 62.42\ \Omega$, $Z_o = 43.27\ \Omega$, and $Z_t = 58.95\ \Omega$. Rogers RT/duroid 6010.2LM high-frequency substrate with thickness of 1.27 mm, a relative permittivity of 10.2, and a loss tangent of 0.0023 was used to fabricate BSF. The BSF was further simulated by Ansys High-Frequency Structure Simulator (HFSS) electromagnetic modeling software to determine the location that could provide maximum sensitivity. As shown in Fig. 1b and 1c, the gaps of CLRs were the regions of highly concentrated electromagnetic field and appropriate position for coating material. Furthermore, the physical parameters of proposed BSF were calculated by ADS software Linecalc tool with $W_0 = 1.2$, $W_1 = 1.0$, $W_2 = 0.8$, $L_1 = 13.8$, $L_2 = 16.6$, and $S_1 = 1.0$ (Units: mm), as shown in Fig. 1d.

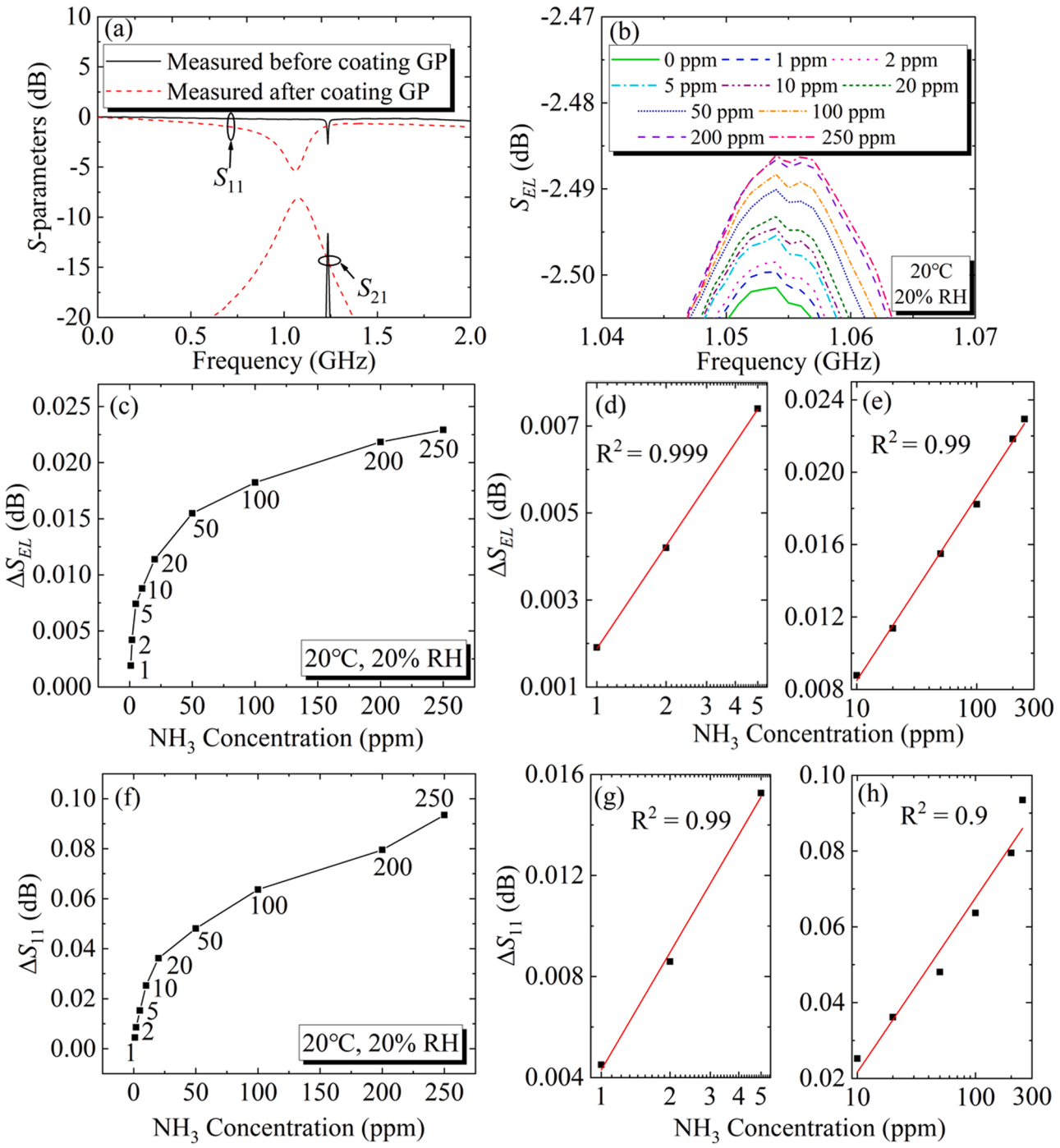

Fig. 2. (a) Measured results of BSF before and after coating GP; (b) S_{EL} and (c) ΔS_{EL} in different concentrations of NH_3 at 20 ℃; the fitting curves of ΔS_{EL} for (d) low NH_3 concentrations (1–5 ppm) and (e) high NH_3 concentrations (10–250 ppm); (f) ΔS_{11} in different concentrations of NH_3 at 20 ℃; the fitting curves of ΔS_{11} for (g) low NH_3 concentrations (1–5 ppm) and (h) high NH_3 concentrations (10–250 ppm).

The photograph of fabricated MGS is shown in Fig. 1e. The commercial GP (Graphite powder, Sinopharm Chemical Reagent Co., 51010760, SP, CAS:7782-42-5) was selected as the sensing material and coated in the gaps of CLR by blade coating method. The SEM image of GP (Fig. 1f) shown a typical layered structure (inset) with particle size from 10 to 40 μm.

All gas sensing tests were performed at room temperature (20 ℃) and 97.79 KPa in a custom 10 L gas chamber (Fig. 1g) by Vector Network Analyzer (VNA, Anritsu MS46122B, Fig. 1h). In this work, the gas response is defined as variation of energy loss at the resonator frequency and can be expressed as

$$\text{Response} = \Delta S_{EL} = S_{EL}^{Targetgas} - S_{EL}^{Air} \quad (1)$$

where S_{EL} is energy loss of the BSF, and can be calculated by

$$|S_{EL}|^2 = 1 - |S_{11}|^2 - |S_{21}|^2 \quad (2)$$

3. Results and discussion

The measured *S*-parameters of BSF before and after coating GP are shown in Fig. 2a. After coating GP, the resonant frequency shifts from 1.234 to 1.054 GHz because of dielectric constant increasing, and the

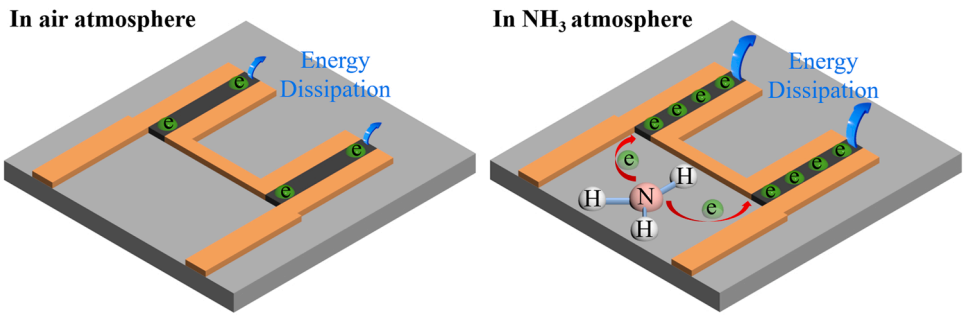

Fig. 3. The schematic diagram of sensing mechanisms of proposed MGS.

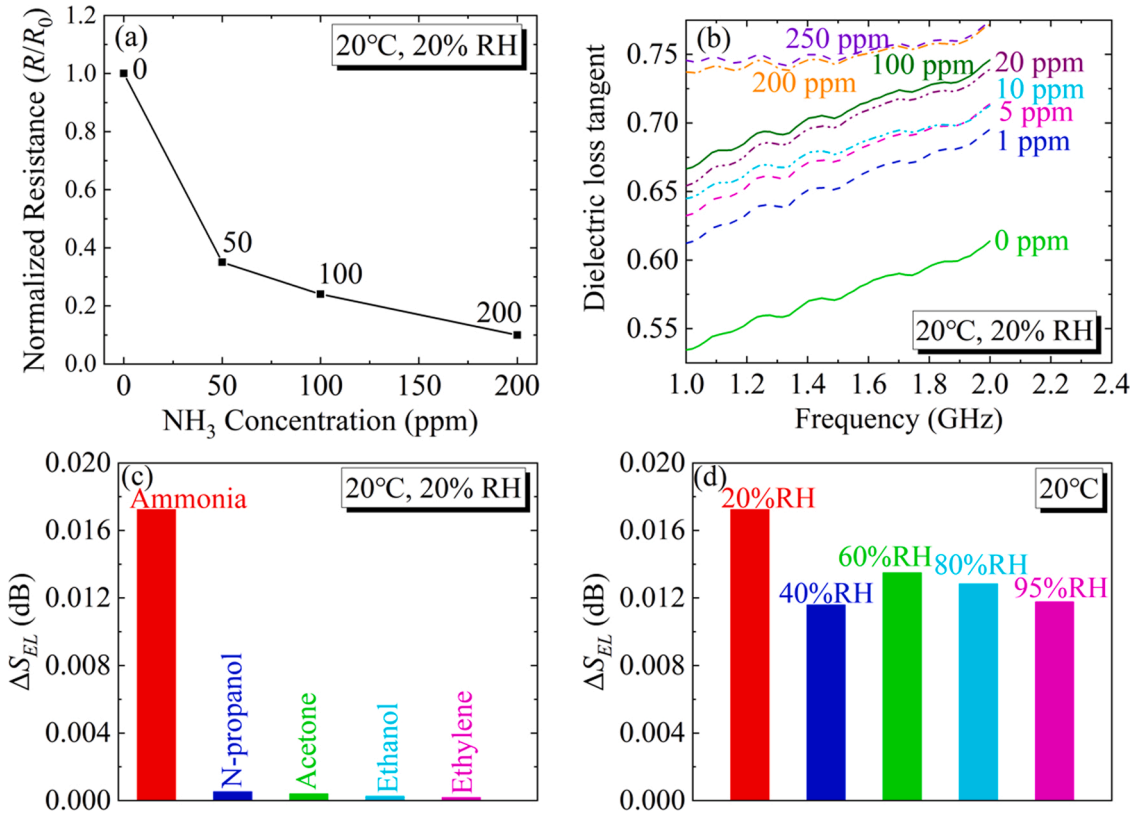

Fig. 4. (a) Resistance value of GP in DC; (b) dielectric loss tangent with the frequency range 1–2 GHz for GP; (c) selectivity of sensor to various gases at the concentration of 50 ppm; (d) the responses of the sensor to 50 ppm NH_3 gas under different relative humidity at 20 ℃.

changes of the amplitude are attributed to energy loss due to the conductivity increase after GP coating. Fig. 2b-c show the S_{EL} and ΔS_{EL} in the NH_3 range from 1 ppm to 250 ppm, respectively. It is obvious that the energy loss will raise with the increase of NH_3 concentrations. Moreover, Fig. 2d-e show the ΔS_{EL} versus low and high NH_3 concentration on the logarithmic scales, indicating that proposed MGS has good linear response. The gas response analyzed by normal method in our previous work are shown in Fig. 2f-h for comparison [10]. It is obvious that the linearity has been significantly enhanced both in low and high NH_3 concentration by the proposed novel analysis method.

The gas response can be attributed to dielectric loss tangent (tanδ) variation of GP. For lossy dielectrics, the permittivity is given by

$$\varepsilon_r = \varepsilon' - j\varepsilon'\prime = \varepsilon' - j\sigma/\omega \tag{3}$$

where ε' and ε'' are the real and imaginary part of permittivity, σ and ω are conductivity and frequency. Moreover, the dielectric loss tangent quantifies dielectric material inherent dissipation of electromagnetic energy and can be expressed as

$$\tan\delta = \varepsilon'\prime/\varepsilon' \tag{4}$$

As illustrated in Fig. 3, electrons would inject into GP due to electron donating nature of NH_3 when GP is exposed to NH_3 environment, and the carrier concentration in GP will increase. Then, the conductivity and tanδ of GP would increase, resulting in the enhanced dissipation of electromagnetic energy in the MGS. The resistance value in DC and the tanδ with frequency range of 1–2 GHz for GP were tested as shown in Fig. 4a and 4b. It is obvious that the conductivity and tanδ of GP are proportional to NH_3 concentration, in accordance with the experimental phenomena and theoretical mechanism discussed above.

In addition to response, selectivity is an important parameter against different gas interference. It can be obviously seen that the sensor displayed highest response to 50 ppm NH_3 as shown in Fig. 4c. Moreover, the humidity influence on the gas response is shown in Fig. 4d. Even though higher humidity values will cause a noticeable reduction in the gas response (32.8%, 21.7%, 25.5%, and 31.7% reduction for 40% RH, 60% RH, 80% RH and 95% RH), the sensor is still capable of sensing the

NH_3.

4. Conclusions

In summary, we rationally designed the MGS based on GP for NH_3 detection, and the results show that the sensor has a low detection limit, excellent selectivity, well linearity, together with good humidity-resistance at room temperature (20 ℃). The gas response can be denoted by the variation of dielectric loss tangent. Moreover, the gas response has firstly adopted variation of energy loss, which was calculated by both transmission and reflection. Based on strong gas adsorption capacity of GP and the novel analysis method, the MGS realized a high response and linearity compared with our previous works [10]. Meanwhile, sensing mechanism has been proposed and verified. This work provides a useful strategy for high-performance MGS fabrication.

CRediT authorship contribution statement

Xiaolong Wang proposed the research direction and guided the project. **Xiaolong Wang, Nan Zhang, Bin Jiang, Shanshan Xue, Tianshuang Wang, Peng Sun and Geyu Lu** conceived and designed the experiments. **Nan Zhang** performed the experiments. **Xiaolong Wang, Nan Zhang, Bin Jiang, Shanshan Xue, Tianshuang Wang, Peng Sun and Geyu Lu** analyzed and discussed the experimental results and wrote the paper.

Declaration of Competing Interest

The authors declare that they have no known competing financial interests or personal relationships that could have appeared to influence the work reported in this paper.

Acknowledgements

This work was supported by Project of Jilin Province People's Government Department of Education, China (Grant No. JJKH20211093KJ), Interdisciplinary Integration and Innovation Project of JLU, China (Grant No. JLUXKJC2020204) and the Project of Science and Technology Bureau of Changchun, China (Grant No. 21ZY23).

References

[1] D. Matatagui, J. López-Sánchez, A. Peña, A. Serrano, A. del Campo, O.R. de la Fuente, et al., Ultrasensitive NO_2 gas sensor with insignificant NH_3-interference based on a few-layered mesoporous graphene, Sens. Actuators B Chem. 335 (2021).
[2] L. Sacco, S. Forel, I. Florea, C.-S. Cojocaru, Ultra-sensitive NO_2 gas sensors based on single-wall carbon nanotube field effect transistors: monitoring from ppm to ppb level, Carbon 157 (2020) 631–639.
[3] X. Wu, X. Yang, F. Zhang, L. Cai, L. Zhang, Z. Wen, Carbon-coated isotropic natural graphite spheres as anode material for lithium-ion batteries, Ceram. Int. 43 (2017) 9458–9464.
[4] K. Shen, X. Chen, W. Shen, Z.-H. Huang, B. Liu, F. Kang, Thermal and gas purification of natural graphite for nuclear applications, Carbon 173 (2021) 769–781.
[5] J.D. Arregui-Mena, R.N. Worth, G. Hall, P.D. Edmondson, A.B. Giorla, T. D. Burchell, A review of finite element method models for nuclear graphite applications, Arch. Comput. Methods Eng. 27 (2018) 331–350.
[6] M.S. Hasan, A. Kordijazi, P.K. Rohatgi, M. Nosonovsky, Machine learning models of the transition from solid to liquid lubricated friction and wear in aluminum-graphite composites, Tribol. Int. 165 (2022).
[7] J.-M. Tulliani, A. Cavalieri, S. Musso, E. Sardella, F. Geobaldo, Room temperature ammonia sensors based on zinc oxide and functionalized graphite and multi-walled carbon nanotubes, Sens. Actuators B Chem. 152 (2011) 144–154.
[8] S.K. Singh, N.K. Tiwari, A.K. Yadav, M.J. Akhtar, K.K. Kar, Design of ZnO/N-doped graphene nanohybrid incorporated RF complementary split ring resonator sensor for ammonia gas detection, IEEE Sens. J. 19 (2019) 7968–7975.
[9] A. Javadian-Saraf, E. Hosseini, B.D. Wiltshire, M.H. Zarifi, M. Arjmand, Graphene oxide/polyaniline-based microwave split-ring resonator: a versatile platform towards ammonia sensing, J. Hazard. Mater. 418 (2021), 126283.
[10] N. Wang, N. Zhang, T. Wang, F. Liu, X. Wang, X. Yan, et al., Microwave gas sensor for detection of ammonia at room-temperature, Sens. Actuators B Chem. 350 (2022).
[11] G. Bailly, J. Rossignol, B. de Fonseca, P. Pribetich, D. Stuerga, Microwave gas sensing with hematite: shape effect on ammonia detection using pseudocubic, rhombohedral, and spindlelike particles, ACS Sens. 1 (2016) 656–662.
[12] G. Bailly, A. Harrabi, J. Rossignol, D. Stuerga, P. Pribetich, Microwave gas sensing with a microstrip interDigital capacitor: detection of NH_3 with TiO_2 nanoparticles, Sens. Actuators B Chem. 236 (2016) 554–564.
[13] G. Bailly, A. Harrabi, J. Rossignol, M. Michel, D. Stuerga, P. Pribetich, Microstrip spiral resonator for microwave-based gas sensing, IEEE Sens. Lett. 1 (2017) 1–4.
[14] J. Rossignol, A. Harrabi, D. Stuerga, P. Pribetich, G. Bailly, T. Leblois, Critical influence of dielectric sensitive material and manufactured process in microwave gas-sensing: application of ammonia detection with an interdigital sensor, ACS Omega 5 (2020) 11507–11514.
[15] W. Krudpun, N. Chudpooti, P. Lorwongtragool, S. Seewattanapon, P. Akkaraekthalin, PSE-coated interdigital resonator for selective detection of ammonia gas sensor, IEEE Sens. J. 19 (2019) 11228–11235.
[16] Y. Liu, B. Sang, H. Wang, Z. Wu, Y. Wang, Z. Wang, et al., High ammonia sensitive ability of novel $Cu_{12}Sb_4S_{13}$ quantum dots@reduced graphene oxide nanosheet composites at room temperature, Chin. Chem. Lett. 31 (2020) 2109–2114.